



Beckham, K.S.H., Byron, O. , Roe, A.J. , and Gabrielsen, M. (2012) The structure of an orthorhombic crystal form of a 'forced reduced' thiol peroxidase reveals lattice formation aided by the presence of the affinity tag. *Acta Crystallographica. Section F: Structural Biology and Crystallization Communications*, 68 (5). pp. 522-526. ISSN 1744-3091

<http://eprints.gla.ac.uk/66789/>

Deposited on: 4th July 2012

Structure of an orthorhombic crystal form of a 'forced reduced' thiol peroxidase reveals lattice formation aided by the presence of the affinity tag

Katherine S H Beckham,^a Olwyn Byron,^b Andrew J Roe^a and Mads Gabrielsen^{a*}

^a*Institute of Infection, Immunity and Inflammation, College of Medical, Veterinary and Life Sciences, Sir Graeme Davies Building, University of Glasgow, G12 8QQ, UK, and*

^b*School of Life Sciences, College of Medical, Veterinary and Life Sciences, Sir Graeme Davies Building, University of Glasgow, G12 8QQ, UK. E-mail: mgabr@chem.gla.ac.uk*

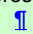
Synopsis The crystal structure of TpxC61S from *E. coli* diffracting to 1.97 Å is reported. A brief structural comparison with homologues is presented.

Abstract Thiol peroxidase (Tpx) is an atypical 2-Cys peroxiredoxin, which has been suggested to be important for cell survival and virulence, in Gram-negative pathogens. The structure of a catalytically inactive version of this protein, in an orthorhombic crystal form, has been determined by molecular replacement. Structural alignments reveal that Tpx is conserved. Analysis of the crystal packing shows that the linker region of the affinity tag is important for the formation of the crystal lattice.

Keywords: Thiol Peroxidase; peroxiredoxin; C61S mutant; reduced

1. Introduction

Thiol peroxidase (Tpx) is an atypical 2-Cys peroxiredoxin found in both Gram-negative and Gram-positive bacteria (Cha *et al.* 1995). Tpx is a redox active protein that reduces alkyl peroxides and hydrogen peroxide through the catalytic recycling of a disulfide bond between cysteines 61 and 95. This cycle results in the production of water with reduced Tpx being regenerated through the interaction with thioredoxin (Baker and Poole 2003). Tpx plays a major contribution to redox homeostasis in the bacterial cell. For example, *Escherichia coli* Tpx deletion mutants display reduced survival after exposure to peroxide (Cha *et al.* 1995). Furthermore this protein has been shown to be important for the survival of human pathogens, such as *Salmonella typhimurium*, where the ability to withstand the oxidative burst in the

The title, authors and addresses contain hidden text. Before editing, reveal the hidden text by pressing  Be sure to preserve the SGML tag structure (see [Help](#))

phagosome is essential (Horst *et al.* 2010). Tpx has also been implicated in the virulence of Gram-negative pathogens, as it was shown to be one of the target proteins of the salicylidene acylhydrazides (Wang *et al.* 2011). These so called “antivirulence” compounds inhibit the bacterial type three secretion system, which is used by pathogens to modulate host cell pathways and facilitate disease (Baron 2010).

Here we describe our crystallization and structure analysis of the catalytically inactive mutant TpxC61S from *E. coli*, which represents a 'forced reduced' structure, as described by (Hall *et al.* 2009). The crystals diffracted to 1.97 Å, and exhibited an orthorhombic form. A brief comparison of this structure with a number of structures of Tpx, present in the Protein Data Bank, including a trigonal crystal form of the same mutant from *E. coli* (Hall *et al.* 2009), is presented. Analysis of the crystal packing of the two TpxC61S structures reveals the importance of parts of the affinity-tag in forming crystal contacts in the orthorhombic space group.

2. Material and methods

2.1. Cloning, expression and purification

The C61S mutant of Tpx was obtained by site directed mutagenesis utilizing a QuickChange Site-Directed Mutagenesis Kit (Stratagene) with the primer pair ecTpx5/3 (CGTACTGATGCGGCCGAAACACCGGTATC and GATACCGGTGTTTCGGCCGCATCAGTACG) with the construct confirmed by DNA sequencing. The amplified product was cloned into the TOPO pET-151 (Invitrogen) expression vector, which encodes an N-terminal affinity tag consisting of a hexahistidine sequence motif with a TEV cleavage site and a linker region consisting of 25 residues. The resulting construct was transformed into BL21 DE3 (λ D3) and grown in 1 L of LB medium containing ampicillin ($100 \mu\text{g ml}^{-1}$). The protein was purified using immobilized metal affinity chromatography protocols as described elsewhere (Gabrielsen *et al.* 2010), and dialysed against 20 mM Tris pH 7.5 and 50 mM NaCl.

2.2. Crystallization

Purified protein with affinity tag, at approximately 8 mg ml⁻¹, was placed into several commercial crystallization screens using sitting drop vapor diffusion, and 1 μl drops in a 1:1 ratio of protein and reservoir. The crystal trays were incubated at 293 K. Crystals appeared in the JCSG+ screen (Molecular Dimensions Ltd) after two weeks against a reservoir of 0.2 M MgCl₂, 0.1 M Tris pH 7 and 10% polyethylene glycol 8000. The crystal was cryo-protected by a short soak in paraffin oil (Riboldi-Tunnicliffe and Hilgenfeld 1999) before being flash-cooled in liquid nitrogen.

2.3. X-ray data measurements, structure solution and refinement

Diffraction data were collected at Diamond Light Source beamline I04 on an ADSC Q315 CCD detector at a wavelength of 0.9763 Å. Data were processed using MOSFLM (Leslie 1992) and scaled and merged using SCALA (Evans 2006) from the CCP4 suite of programs (Winn *et al.* 2011). The structure of C61S was determined using PHASER, and the existing C61S structure from *E. coli*, (PDB code 3HVV) (Hall *et al.* 2009) was used as a search model, for molecular replacement. The structure was refined using REFMAC5 (Murshudov *et al.* 1997) and BUSTER (Bricogne *et al.* 2011). The model was manipulated as required, and waters were added using COOT (Emsley *et al.* 2010). The model was validated using COOT and the Molprobit server (Davis *et al.* 2007). PISA was used to analyze protein interfaces and crystal contacts (Krissinel and Henrick 2007) and structural superpositions were performed using the SUPER command in PYMOL (Schrödinger 2012). Figures were made using ALINE (Bond and Schüttelkopf 2009) and PymOL.

The structure and data were deposited into the Protein Data Bank (Velankar *et al.* 2012) (accession code 4AF2).

3. Results and Discussion

3.1. Crystallization, data collection and structure determination

The crystals of the C61S mutant of Tpx from *E. coli* were orthorhombic, with dimensions of approximately 0.1 x 0.1 x 0.03 mm (Figure 1A), and exhibited space group $C222_1$, with unit cell parameters of $a = 49.37$, $b = 71.75$, $c = 121.93$ Å. The data were collected to a resolution of 1.97 Å (Figure 1B), and the relevant data collection statistics are presented in Table 1. The asymmetric unit comprised one subunit with a Matthews coefficient of $3.09 \text{ \AA}^3 \text{ Da}^{-1}$, indicating a solvent content of 60%. The data processed well, with overall R_{meas} and R_{pim} values of 14.2% and 5.7 % respectively.

The molecular replacement solution was refined to final R_{work} and R_{free} factors of 22.9% and 28.3%, respectively. There are no outliers in the Ramachandran plot, and the structure is in the 94th percentile of Molprobit clash scores (Davis *et al.* 2007). All relevant structure refinement statistics are listed in Table 1.

3.2. Overall structure of TpxC61S

TpxC61S exhibits a thioredoxin-like fold, with a seven-stranded β -sheet, flanked by four α helices, with an additional two N-terminal β -strands typical for Tpx but not found in other peroxiredoxin structures (Figure 2). Due to the mutation of the active cysteine residue to a

serine, the structure is locked in the reduced confirmation. This conformation has an elongated $\alpha 1$ helix, which makes C61 available for interactions with H_2O_2 or alkyl peroxides, however the presence of the mutation to serine prevents these interactions. Following oxidation of C61 helix $\alpha 1$ becomes unraveled to form an intramolecular disulfide bond with residue C95 (Hall *et al.* 2009; Gabrielsen *et al.* 2012). The conformational change observed in response to redox state is show in Figure 3B.

Tpx forms a homodimer in solution (Baker and Poole 2003; Gabrielsen *et al.* 2012). In this crystal structure the dimer is formed by a crystallographic symmetry related molecule. The structure of TpxC61S superposes well onto other crystal structures of reduced structures of Tpx (Table 2). In particular, this mutant superposes with the wild-type reduced protein from *Yersinia pseudotuberculosis* (Gabrielsen *et al.* 2012) with a root-mean-squared-deviation (rmsd) of 0.376 Å indicating a high degree of similarity (Figure 3A). This confirms the assumption made by Hall *et al.* that TpxC61S represents a ‘forced reduced’ structure. When compared with the oxidized *E. coli* structure (3HVS) (Hall *et al.* 2009), TpxC61S superposed with an rmsd of 0.711 Å. This reflects the local conformational change between the oxidized and reduced structure mediated by the formation of a disulfide bond between C61 and C95 (Figure 3B).

3.3. Analysis of the crystal lattice

The orthorhombic form of TpxC61S superposes well onto the existing, trigonal TpxC61S structure (3HVV) (Hall *et al.* 2009) with an rmsd of 0.207 Å, showing that despite the different space groups, $C222_1$ versus $P3_121$ respectively, the structure remains essentially the same (Figure 2B). However, when investigating the crystal packing, a noticeable difference between the two crystal forms became apparent. The unit cell of the trigonal form of TpxC61S is much more densely packed, with a solvent content of 42%. In contrast, orthorhombic TpxC61S has a solvent content of 60%. This explains the difference in crystal contacts formed between the monomeric asymmetric unit and its environment. Whilst the trigonal crystal form has ten neighboring TpxC61S within 5.0 Å, the orthorhombic form has only six.

Despite the more spacious packing of the protein in $C222_1$, the crystals diffract similarly and are robust. When analyzing the crystal lattice, the linker region of the affinity tag construct, accounted for in the electron density, in orthorhombic TpxC61S, is involved in several crystal contacts, and thus stabilizes the crystal through facilitating lattice formation (Figure 4A).

Analysis of the crystal packing in the orthorhombic crystal lattice, using the Protein Interfaces, Surfaces and Assemblies Server (PISA) (Krissinel and Henrick 2007), revealed that of a total surface area of 8349 Å², 17% of this was buried. The largest buried area occurs

at the dimerisation interface of the protein, which accounts for about half of the buried surface area. The rest of the crystal contacts are formed between the linker region of the affinity tag of one molecule with a neighboring molecule, shown in Figure 4B, and a smaller second crystal contact with another subunit. The area of contact conferred by the linker region is stabilized by two hydrogen bonds between the tag (I-4 and F-1) and a symmetry related molecule (K'33) (Figure 3B). In comparison, the buried surface area between trigonal TpxC61S and the symmetry related neighbors makes up around 10% of the total surface area. However, each subunit has direct crystal contacts with 8 symmetry related molecules. This highlights the importance of the tag in stabilizing TpxC61S in the orthorhombic form.

4. Conclusions

We have reported the structure of an orthorhombic crystal form of TpxC61S from *E. coli* at 1.97 Å. The overall structure is well conserved amongst the known homologues, and this mutant form is a good representation of the reduced form of Tpx. The crystal lattice is held in place by the linker region of the affinity-tag of one subunit attaching to a neighboring unit, threading the lattice throughout.

Figure 1 *Escherichia coli* TpxC61S crystals and diffraction. A) The orthorhombic crystals have dimensions of 0.1 x 0.1 x 0.3 mm. B) The crystals diffracted to 1.97 Å (at detector edge) and exhibited space group $C222_1$.

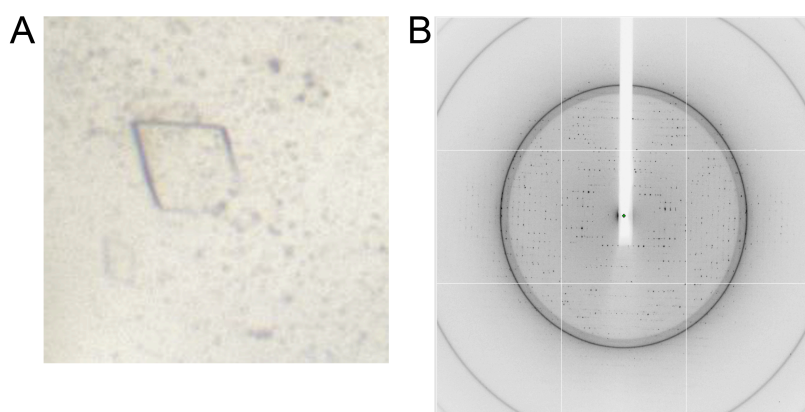


Figure 2 The structure of orthorhombic TpxC61S compared with existing structures. A) The overall structure of TpxC61S is shown with serine 61 (red) and cysteine 95 (yellow) highlighted. The N- and C-terminal of the protein have been labeled, along with the secondary structure elements. B) The sequence of the purified and crystallized protein with secondary elements above, and the catalytic residues highlighted. The affinity tag is shown in grey, with the part of the tag that can be observed in electron density in pink.

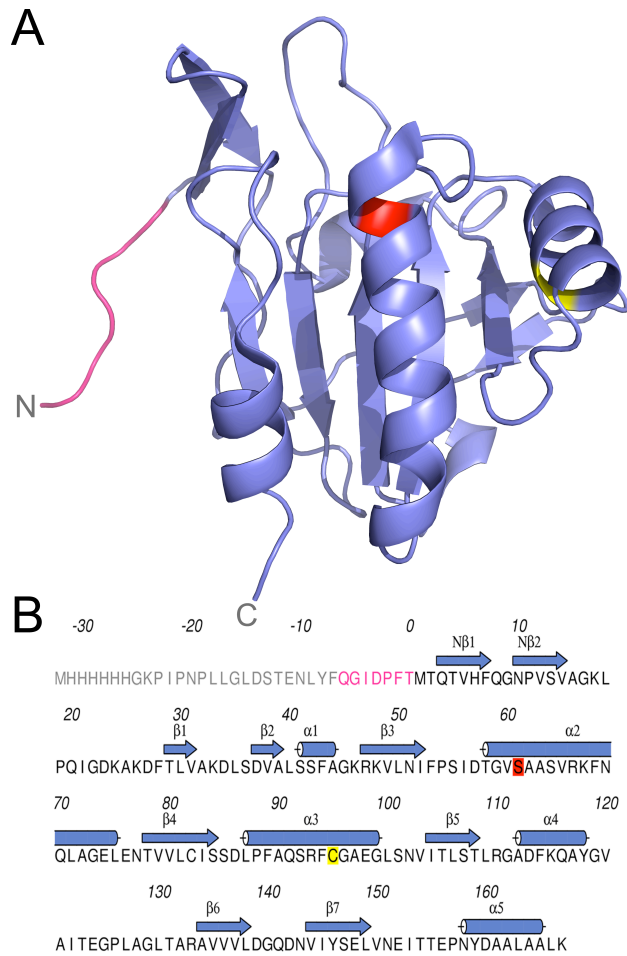


Figure 3 Comparison of TpxC61S with existing Tpx structures. A) Superposition of orthorhombic TpxC61S (slate) with trigonal TpxC61S (PDB code 3HVV) (Hall *et al.* 2009) (pink) (from *E. coli*) and reduced wild type Tpx (PDB code 2XPD)(Gabrielsen *et al.* 2010) (green) (from *Y. pseudotuberculosis*) illustrates the high level of similarity between this and the existing TpxC61S structure from *E. coli*, and reduced wild-type Tpx. B) Orthorhombic TpxC61S (slate) superimposes less well with oxidised wild-type Tpx (cyan) (PDB code 3HVS) (Hall *et al.* 2009) due to the conformational change caused by differing redox states.

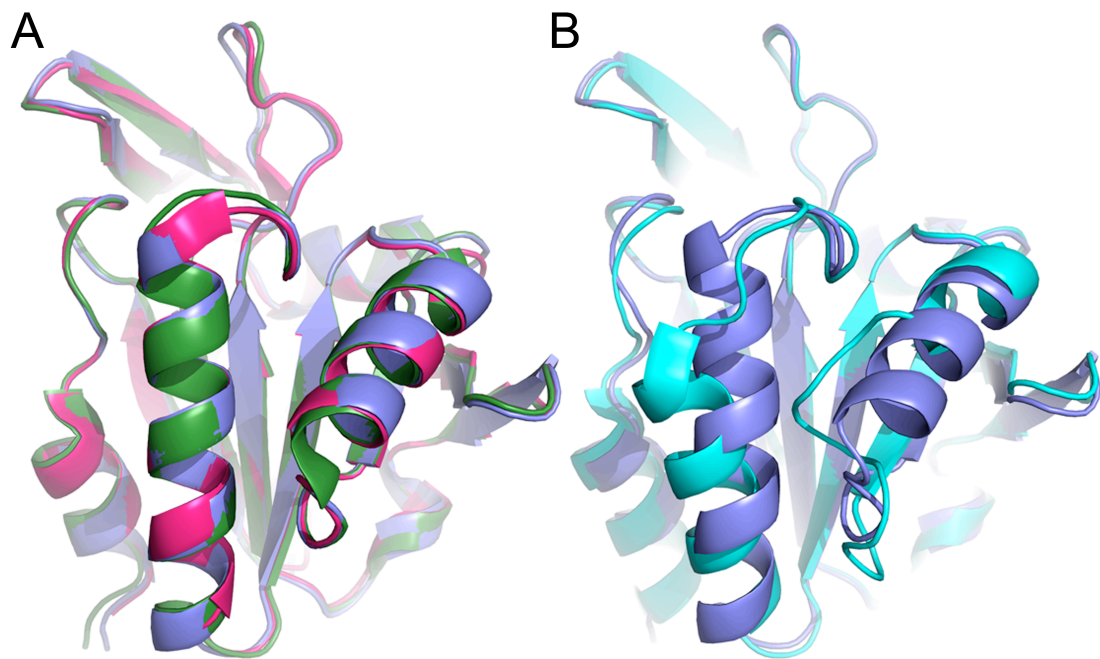


Figure 4 Crystal packing of TpxC61S. A) The crystal lattice formed in the orthorhombic crystal form of TpxC61S highlights the importance of the linker region of the affinity-tag (pink) in forming crystal contacts. The biological dimer, formed by crystallographic symmetry, has been shown in slate with other molecules in the crystal lattice in light blue. B) Inset is a detailed view of the crystal contacts between the linker region and a symmetry related molecule highlighted in the black box shown in A. Residues involved in hydrogen bond formation have been labeled, namely K'33 N ζ to I -4 N (3.2 Å) and K'33 O to F -1 O (3.1 Å). The hydrogen bonds are shown as dashed lines.

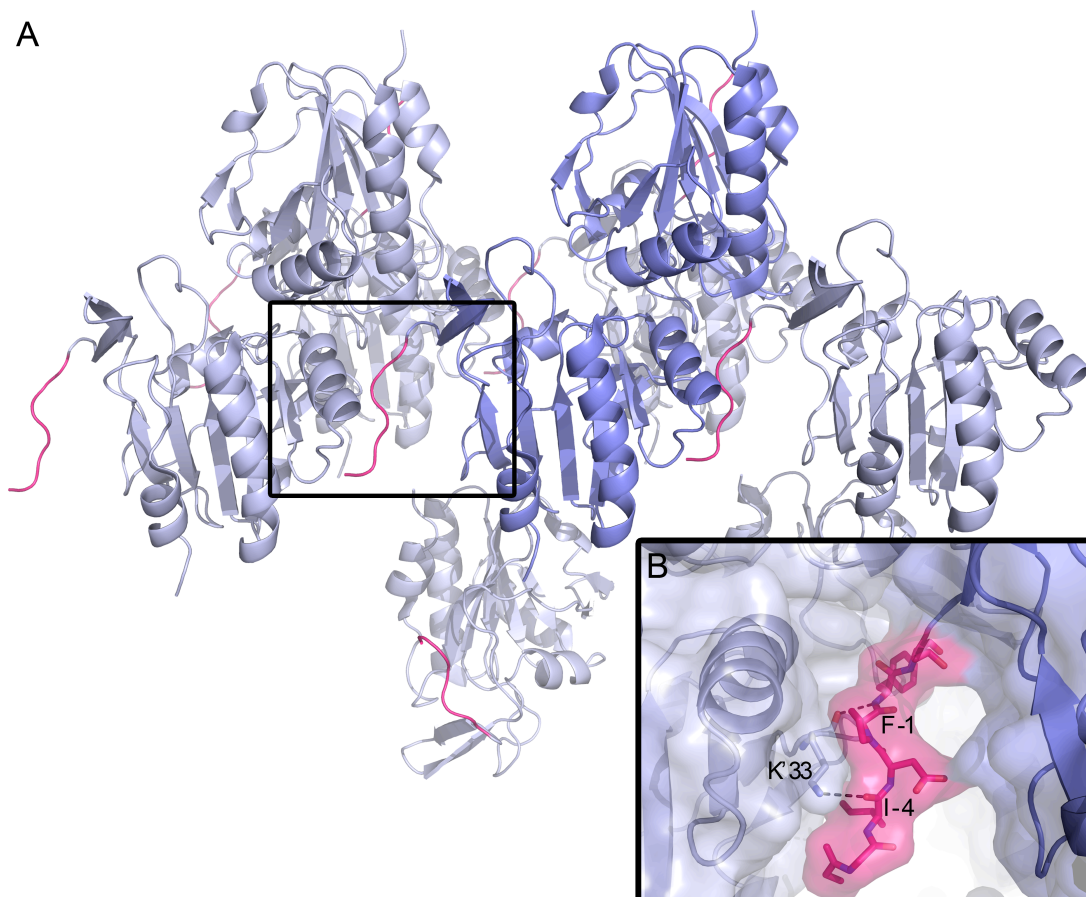


Table 1 Data collection and refinement statistics. Numbers in brackets show data for the highest resolution

PDB code	4A2F
Space group	$C222_1$
Unit cell parameters (Å)	$a = 49.37, b = 71.75, c = 121.93$
Resolution (Å)	40.67 - 1.97 (2.08 - 1.97)
Observed reflections	96980
Unique reflections	15679
Multiplicity	6.2 (6.6)
Completeness (%)	90.2 (100)
R_{meas}^* (%)	14.2 (67.5)
$R_{\text{pim}}^{\#}$ (%)	5.7 (26.0)
$(I/\sigma(I))$	7.5 (2.8)
Wilson B (Å ²)	19.9
Matthews (Å ³ Da ⁻¹)	3.09
Solvent content (%)	60.16
Water oxygen atoms	170
R_{work} (%)	22.93

R_{free} (%)	28.28
Rmsd for bond lengths (Å) / angles (°)	0.009 / 1.17
Average isotropic thermal parameters (Å ²)	
Main chain	35.34
Side chain	40.95
Water oxygen atoms	37.53
Ramachandran outliers (%)	0
Molprobrity clash score	6.57 [94th percentile]

$$^*R_{\text{meas}} \text{ is defined as } \sum_h \sum_l \left(\frac{n_h}{n_h - 1} \right)^{1/2} |I_{hl} - \langle I_h \rangle| / \sum_h \sum_l \langle I_h \rangle$$

$$^{\#}R_{\text{pim}} \text{ is defined as } \sum_h \sum_l \left(\frac{1}{n_h - 1} \right)^{1/2} |I_{hl} - \langle I_h \rangle| / \sum_h \sum_l \langle I_h \rangle$$

Table 2 Superposition of orthorhombic TpxC61S with reduced wild type and 'forced reduced' mutated Tpx structures. The oxidized Tpx from *Escherichia coli* (3HVS) has been added for completeness.

Species	PDB code
<i>Escherichia coli</i>	3HVV
<i>Yersinia psuedotuberculosis</i>	2XPD
<i>Y. psuedotuberculosis</i>	2YJH
<i>Mycobacterium tuberculosis</i>	1Y25
<i>Streptococcus pneumoniae</i>	1PSQ
<i>E. coli</i>	3HVS

Acknowledgements We thank Diamond Light Source for access to beamline I04 (proposal number MX1229). The work was supported by a grant from the Biotechnology and Biological Sciences Research Council to MG and AJR (BB/G011389/1), a Medical Research Scotland Grant (223 ORG) to AJR, and a Wellcome Trust Studentship for KSHB. We acknowledge Karen McLuskey for discussions and thorough reading of the manuscript.

References

- Baker, L. M. and L. B. Poole (2003). *J Biol Chem* **278**: 9203-9211.
- Baron, C. (2010). *Curr Opin Microbiol* **13**: 100-105.
- Bond, C. S. and A. W. Schüttelkopf (2009). *Acta Crystallogr D Biol Crystallogr* **65**: 510-512.
- BUSTER version 2.8.0, Bricogne, G., E. Blanc, M. Brandl, C. Flensburg, P. Keller, W. Paciorek, P. Roversi, A. Sharff, C. Vonrhein and T. O. Womack, 2011,
- Cha, M. K., H. K. Kim and I. H. Kim (1995). *J Biol Chem* **270**: 28635-28641.
- Davis, I. W., A. Leaver-Fay, V. B. Chen, J. N. Block, G. J. Kapral, X. Wang, L. W. Murray, W. B. Arendall, 3rd, J. Snoeyink, J. S. Richardson and D. C. Richardson (2007). *Nucleic Acids Res* **35**: W375-383.
- Emsley, P., B. Lohkamp, W. G. Scott and K. Cowtan (2010). *Acta Crystallogr D Biol Crystallogr* **66**: 486-501.
- Evans, P. (2006). *Acta Crystallogr D Biol Crystallogr* **62**: 72-82.
- Gabrielsen, M., K. S. H. Beckham, V. A. Feher, C. Z. Zetterstrom, D. Wang, S. Muller, M. Elofsson, R. E. Amaro, O. Byron and A. J. Roe (2012). *PLoS ONE* **7**: e32217.
- Gabrielsen, M., C. E. Zetterstrom, D. Wang, K. S. Beckham, M. Elofsson, N. W. Isaacs and A. J. Roe (2010). *Acta Crystallogr Sect F Struct Biol Cryst Commun* **66**: 1606-1609.
- Hall, A., B. Sankaran, L. B. Poole and P. A. Karplus (2009). *J Mol Biol* **393**: 867-881.
- Horst, S. A., T. Jaeger, L. A. Denkel, S. F. Rouf, M. Rhen and F. C. Bange (2010). *J Bacteriol* **192**: 2929-2932.
- Krissinel, E. and K. Henrick (2007). *Journal of Molecular Biology* **372**: 774-797.
- Leslie, A. G. W. (1992). *Joint CCP4 + ESF-EAMCB Newsletter on Protein Crystallography* **26**.
- Murshudov, G. N., A. A. Vagin and E. J. Dodson (1997). *Acta Crystallographica Section D-Biological Crystallography* **53**: 240-255.
- Riboldi-Tunncliffe, A. and R. Hilgenfeld (1999). *Journal of Applied Crystallography* **32**: 1003-1005.
- The PyMOL Molecular Graphics System, Version 1.5.0.1, Schrödinger, L., 2012, www.pymol.org
- Velankar, S., Y. Alhroub, C. Best, S. Caboche, M. J. Conroy, J. M. Dana, M. A. Fernandez Montecelo, G. van Ginkel, A. Golovin, S. P. Gore, A. Gutmanas, P. Haslam, P. M. Hendrickx, E. Heuson, M. Hirshberg, M. John, I. Lagerstedt, S. Mir, L. E. Newman, T. J. Oldfield, A. Patwardhan, L. Rinaldi, G. Sahni, E. Sanz-Garcia, S. Sen, R. Slowley, A. Suarez-Uruena, G. J. Swaminathan, M. F. Symmons, W. F. Vranken, M. Wainwright and G. J. Kleywegt (2012). *Nucleic acids research* **40**: D445-452.
- Wang, D., C. E. Zetterstrom, M. Gabrielsen, K. S. Beckham, J. J. Tree, S. E. Macdonald, O. Byron, T. J. Mitchell, D. L. Gally, P. Herzyk, A. Mahajan, H. Uvell, R. Burchmore, B. O. Smith, M. Elofsson and A. J. Roe (2011). *The Journal of biological chemistry* **286**: 29922-29931.
- Winn, M. D., C. C. Ballard, K. D. Cowtan, E. J. Dodson, P. Emsley, P. R. Evans, R. M. Keegan, E. B. Krissinel, A. G. W. Leslie, A. McCoy, S. J. McNicholas, G. N. Murshudov, N. S. Pannu, E. A. Potterton, H. R. Powell, R. J. Read, A. Vagin and K. S. Wilson (2011). *Acta Crystallographica Section D-Biological Crystallography* **67**: 235-242.